Phase Transitions Occurring upon Lithium Insertion−Extraction of $LiCoPO_4$

Natalia N. Bramnik,*,† Kristian Nikolowski,† Carsten Baehtz,‡ Kirill G. Bramnik,† and Helmut Ehrenberg†

Institute for Materials Science, University of Technology, Petersenstrasse 23, 64287 Darmstadt, Germany, and Hasylab/DESY, Notkestrasse 85, D-22607 Hamburg, Germany

Received September 19, 2006. Revised Manuscript Received November 10, 2006

In situ synchrotron diffraction revealed a stepwise appearance of two new phases upon electrochemical lithium extraction from $LiCoPO_4$. These phases were demonstrated to have the same olivine-like structure as the pristine compound. The lithium-deficient phases were proposed to be $Li_{0.7}CoPO_4$ and $CoPO_4$. The completely delithiated phase appears to be unstable in air and undergoes amorphization. The phase transitions are reversible, but a slow kinetics of the initial delithiation was identified by in situ synchrotron diffraction and the potentiostatic intermittent titration technique. We demonstrated that the electrochemical extraction of lithium is accompanied by significant electrolyte decomposition, contributing to the capacity loss upon cycling. The galvanostatic intermittent titration technique combined with impedance spectroscopy revealed self-discharge of the cell in the charged state. This study argues different mechanisms of lithium extraction from $LiCoPO_4$ in comparison with $LiFePO_4$ and $LiMnPO_4$.

Introduction

The development and commercialization of the low-cost and stable $LiFePO_4$ cathode for lithium-ion batteries provoked strong interest in the other members of the olivine-like metallophosphates family Li*M*PO_4 (*M* = Mn, Fe, Co, Ni).[1−4] The electrochemical reaction of lithium extraction from $LiFePO_4$ and $LiMnPO_4$ leads to the formation of completely delithiated compounds; both phases pristine Li*M*PO_4 and appearing *M*PO_4 (space group *Pnma*) are isostructural with different cell parameters.[5−7] Recently, Yamada et al. demonstrated that this simple model for the delithiation of $LiFePO_4$ should be corrected.[8] A careful X-ray powder diffraction revealed two narrow monophase regions ($0 < x < \alpha$ and $1-\beta < x < 1$, $\alpha = 0.032$, $\beta = 0.038$ at room temperature) close to the end members $LiFePO_4$ and $FePO_4$. These results are supported by a neutron diffraction study[9] and consistent with the reaction model proposed by Srinivasan and Newman.[10] According to this model, the intermediate composition Li_xFePO_4 consists of a mixture of $Li_\alpha FePO_4$ and $Li_{1-\beta}FePO_4$ phases, where α and β depend on temperature, particle size, and doping.

The structure evolution during delithiation of $LiCoPO_4$ is not completely resolved yet. Amine at al. reported the formation of a second olivine-like phase upon lithium extraction from $LiCoPO_4$.[1] A two-phase mechanism of lithium extraction from $LiCoPO_4$ was confirmed by in situ synchrotron diffraction.[11] The difference in the cell volumes between pristine and delithiated phases was reported to be about 2%, which is much lower in comparison with $LiFePO_4$/$FePO_4$ (7%) and $LiMnPO_4$/$MnPO_4$ (8.9%).[6,7] On the other hand, ex situ diffraction on other $LiCoPO_4$ samples annealed at low temperatures showed a pronounced amorphization of the cathode material after electrochemical delithiation.[12] An amorphization of the cathode material was also observed upon chemical oxidation of $LiCoPO_4$ with NO_2BF_4.[13]

An additional discrepancy in the literature concerns the character of the voltage−composition curves reported for $LiCoPO_4$. The cyclic voltammetry for this compound revealed only one oxidation (5.1 vs Li/Li^+) and one reduction peak (4.8 V vs Li/Li^+), which are characteristic for a reversible one-step electrochemical process.[1] In contrast to the voltage−composition curves reported for $LiCoPO_4$,[1,14−16]

* Corresponding author. Phone: 49 (0)6151 166359. Fax: 49 (0)6151 166023. E-mail: bramnik@tu-darmstadt.de.
† University of Technology.
‡ Hasylab/DESY.

(1) Amine, A.; Yasuda, H.; Yamachi, M. *Electrochem. Solid State Lett.* **2000**, *3*, 178.
(2) Okada, S.; Sawa, S.; Egashira, M.; Yamaki, J.; Tabuchi, M.; Kageyama, H.; Konishi, T.; Yoshino, A. *J. Power Sources* **2001**, *97*−*98*, 430.
(3) Delacourt, C.; Wurm, C.; Realle, P.; Morcrette, M.; Masquelier, C. *Solid State Ionics* **2004**, *173*, 113.
(4) Kwon, N.; Drezen, T.; Exnar, I.; Teerlinck, I.; Isono, M.; Gtaetzel, M. *Electrochem. Solid State Lett.* **2006**, *9*, A277.
(5) Padhi, A.; Nanjundaswamy, K.; Goodenough, J. *J. Electrochem. Soc.* **1997**, *144*, 1188.
(6) Andersson, A.; Kalska, B.; Häggström, L.; Thomas, J. *Solid State Ionics* **2000**, *130*, 41.
(7) Delacourt, C.; Poizot, P.; Morcrette, M.; Tarascon, J.-M.; Masquelier, C. *Chem. Mater.* **2004**, *16*, 93.
(8) Yamada, A.; Koizumi, H.; Sonoyama, N.; Kanno, R. *Electrochem. Solid State Lett.* **2005**, *8*, A409.
(9) Yamada, A.; Koizumi, H.; Nishimura, S;, Sonoyama, N.; Kanno, R.; Yonemura, M.;. Nakamura, T.; Kobayashi, Y. *Nat. Mater.* **2006**, *5*, 357.
(10) Srinivasan, V.; Newman, J. *J. Electrochem. Soc.* **2004**, *151*, A1517.
(11) Bramnik, N. N.; Bramnik, K. G.; Baehtz, C.; Ehrenberg, H. *J. Power Sources* **2005**, *145*, 74.
(12) Bramnik, N. N.; Bramnik, K. G.; Buhrmester, T.; Baehtz, C.; Ehrenberg, H.; Fuess, H. *J. Solid State Electrochem.* **2004**, *8*, 558.
(13) Wolfenstine, J.; Poese, B.; Allen, J. *J. Power Sources* **2004**, *138*, 281.
(14) Eftekhari, A. *J. Electrochem. Soc.* **2004**, *151*, A1456.
(15) Deniard, P.; Dulac, A. M.; Rocquefelte, X.; Grigorova, V.; Lebacq, O.; Pasturel, A.; Jobic, S. *J. Phys. Chem. Solids* **2004**, *65*, 229.

10.1021/cm062246u CCC: $37.00
Published on Web 01/17/2007

we observed a two-step character of the electrochemical reaction reflected by two plateaus during galvanostatic charge−discharge.[11,12] The existence of two steps during lithium extraction−insertion was unambiguously identified with PITT cycling. We have shown that two oxidation (4.8 and 4.9 V vs Li/Li+) and two reduction peaks (4.7 and 4.8 V vs Li/Li+) in the incremental capacity plot are more pronounced for the second and following cycles. Additionally, the voltage difference between corresponding oxidation−reduction peaks is higher upon initial charge−discharge than in following cycles, indicating a higher polarization in the first cycle in comparison with successive ones.[11]

Recently, the existence of two plateaus at $0.7 \leq x \leq 1$ and $0 \leq x \leq 0.7$ in Li_xCoPO_4 in the charge process was confirmed by Nakayama et al.[17] It was shown that both plateaus are related to the lithium removal accompanied by the Co oxidation in the entire region of charge (from $0 \leq x \leq 1$). On the basis of X-ray absorption spectroscopy experiments, the authors concluded that the electronic configurations of P and O vary as well as electronic configurations of Co ions with electrochemical charging.[18] This study indicated that the two-step behavior cannot be ascribed to side reactions of electrolyte degradation occurring in the high-voltage range and should be considered as being intrinsic property of this material. Nevertheless, the origin of two plateaus was not clarified.

In this paper, we report for the first time that the two-step character of lithium extraction−insertion from $LiCoPO_4$ is related to the existence of two two-phase regions. We characterize the electrochemical extraction−insertion of this compound by electrochemical methods PITT, GITT, and impedance spectroscopy. In situ synchrotron diffraction performed for the complete charge−discharge cycle unambiguously proves the stepwise phase separation upon lithium extraction from this compound.

Experimental Section

$LiCoPO_4$ was prepared by solid-state reaction of stoichiometric amounts of CoO (Aldrich, 99,9%), Li_2CO_3 (Aldrich, 99%), and $(NH_4)_2HPO_4$ (Aldrich, 99,8%). Acetylene carbon black (99.99%, 100% compressed, STREM Chemicals) was added to the reactants to minimize particle size during synthesis and to provide better electronic contact between the $LiCoPO_4$ particles (5% w/w). The initial calcination was performed at 500 °C for 12 h in argon flow. After additional ball-milling and pelletizing, the mixture was annealed for 24 h in an argon atmosphere at 600 °C. The final product contains 6.1% w/w carbon determined by elemental analysis (Elementar VarioEL III analyzer). The average particle size determined by laser diffraction (Fritsch analyzette 22 compact) is 0.8 μm. The olivine-like crystal structure and phase purity of the product was confirmed by XRD using a STOE STADI/P powder diffractometer (Mo $K\alpha_1$ radiation, curved Ge (111) monochromator, transmission mode, step width 0.02° (2θ), linear PSD counter).

Electrochemical experiments were carried out with a multichannel potentiostatic−galvanostatic system VMP (Perkin-Elmer Instruments, United States). The complex cell impedance was measured with an AC modulation amplitude of 10 mV in the frequency range from 100 kHz to 5 mHz. Swagelok-type cells were assembled in an argon-filled dry box with water and oxygen contents less than 1 ppm. The cathode composite consisted of 75% active material, 20% acetylene carbon black, and 5% polyvinylidene fluoride as polymer binder. To prepare the cathode, we added all components to *N*-methylpyrrolydon and cast this slurry on Al foil. After being dried, it was punched into circular discs (diameter 8 mm with a loading of about 1 mg of active material). In all experiments, a lithium anode, glass-fiber separator, and liquid electrolyte (1 M $LiPF_6$ in 2:1 EC:DMC vol %, Ferro) were used. A Swagelok-type electrochemical cell was used for in situ synchrotron diffraction.[19] In this case, the cathode mixture was pressed as a pellet (about 30 mg, 10 mm diameter). The cell was mounted on a flat sample holder that was oscillated to reduce preferred orientation effects in powder statistics. The on-site readable image-plate detector "OBI" collected the whole diffraction pattern within an exposure time of about 10−15 min.[20] Structure refinement was performed by the Rietveld method using the Winplotr software package.[21]

Results and Discussions

The galvanostatic ($C/6$) charge−discharge of the cell with $LiCoPO_4$ cathode reveals a high capacity loss in the first cycle, which is consistent with previous data reported for this compound (see Figure 1).[1,2,11,12,16] After being charged to the composition "$CoPO_4$", the cell delivers about 60% of the theoretical capacity (166 mA h^{-1} g^{-1}). The lithium extraction−insertion in $LiCoPO_4$ was demonstrated to proceed in a reversible manner. Amine et al. reported that the diffraction pattern of the material after one complete cycle is very similar to the one of the pristine compound.[1] This result indicates that the capacity loss in the first cycle cannot be attributed to the irreversible phase transitions occurring upon cycling. The limited electronic/ionic transport, well-known for olivine-type metallophosphates, can contribute to the loss in capacity.[22,23] In this case, the discharge capacity should increase at low current rates. As we reported previously, upon galvanostatic cycling at low current density (lower than $C/6$), the electrochemical performance of $LiCoPO_4$ deteriorates.[11] This behavior was explained by the contribution of the electrolyte decomposition, which is more significant at slow charging of the cell. In fact, the thermodynamic instability of the electrolyte at the operation voltage close to 5 V vs metallic lithium could be the reason for this drastic capacity loss. If a side reaction upon charging of the cell occurs, it contributes to the charge passed through the cell and then biases the calculation of the amount of extracted lithium. The "real" amount of lithium extracted upon the charge could be lower than the calculated one. On the other hand, the degradation of the electrolyte on the

(16) Lloris, J.; Pérez Vicente, C.; Tirado, J. *Electrochem. Solid State Lett.* **2002**, *5*, A234.
(17) Nakayama, M.; Goto, S.; Uchimoto, Y.; Wakihara, M.; Kitayama, Y. *Chem. Mater.* **2004**, *16*, 3399.
(18) Nakayama, M.; Goto, S.; Uchimoto, Y.; Wakihara, M.; Kitayama, Y.; Miyanaga, T.; Watanabe, I. *J. Phys. Chem. B* **2005**, *109*, 11197.
(19) Nikolowski, K.; Baehtz, C.; Bramnik, N. N.; Ehrenberg, H. *J. Appl. Cryst.* **2005**, *38*, 851.
(20) Knapp, M.; Joko, V.; Baehtz, C.; Brecht, H.; Berghauser, A.; Ehrenberg, H.; von Seggern, H.; Fuess, H. *Nucl. Instrum. Methods Phys. Res., Sect. A* **2004**, *521*, 565.
(21) Roisnel, T.; Rodriguez-Carvajal, J. *Mater. Sci. Forum* **2001**, *378*, 118.
(22) Yonemura, M.; Yamada, A.; Takei, Y.; Sonoyama, N.; Kanno, R. *J. Electrochem. Soc.* **2004**, *151*, A1352.
(23) Delacourt, C.; Laffont, L.; Bouchet, R.; Wurm, C.; Leriche, J.-B.; Morcrette, M.; Tarascon, J.-M.; Masquelier, C. *J. Electrochem. Soc.* **2005**, *152*, A913.

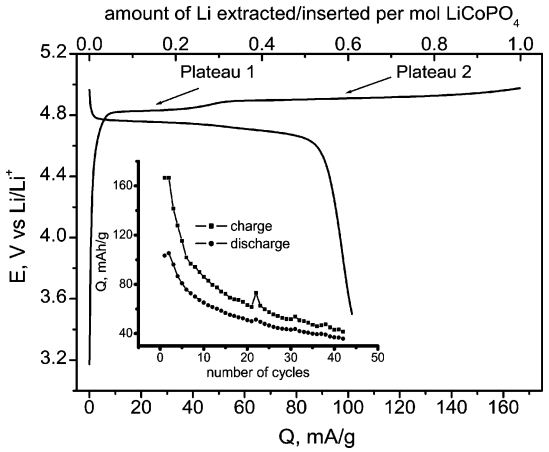

Figure 1. Voltage profile during the first galvanostatic (*C*/6) charge−discharge of the $LiCoPO_4$ cell. Insert: Capacity decay upon cycling.

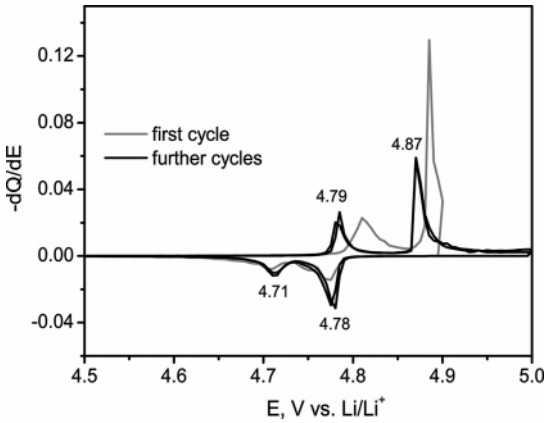

Figure 2. Incremental capacity plot obtained by potentiodynamic cycling with I_{lim} close to *C*/12 ($\Delta E = 5$ mV).

cathode side may cause a limitation in mass transport on the cathode/electrolyte interface.

The existence of two plateaus ($0.7 \leq x \leq 1$ and $0 \leq x \leq 0.7$) in the charge curve is clearly illustrated in Figure 1. The same electrochemical behavior was observed with another electrolyte system (lithium bis(oxalate)borate in EC/EMC, Chemetall GmbH) (data not shown). This supports the idea that two-step delithiation is intrinsic property of this compound and cannot be ascribed to the parasitic reactions. Two steps during discharge are not resolved in galvanostatic cycling, but can be clearly identified in the PITT experiment performed with accelerating current close to *C*/12 (see Figure 2). In agreement with previous data, two steps during charge−discharge are more pronounced for the second and following cycles. Both oxidation peaks in the initial cycle are shifted to more positive voltages in comparison with further cycles. This behavior indicates the slow kinetic of the initial delithiation of $LiCoPO_4$. In general, the current at the end of a voltage step in a PITT experiment (I_{lim}) should be very small to approximate equilibrium state conditions. Conducting the PITT experiment with I_{lim} close to *C*/30, we observed a number of oxidation peaks in the incremental capacity curve in the first cycle (Figure 3). Nevertheless, the plot in the fourth cycle is very similar to the plot for further cycles shown in Figure 2. The difference between the oxidation−reduction peaks is the same in both cases.

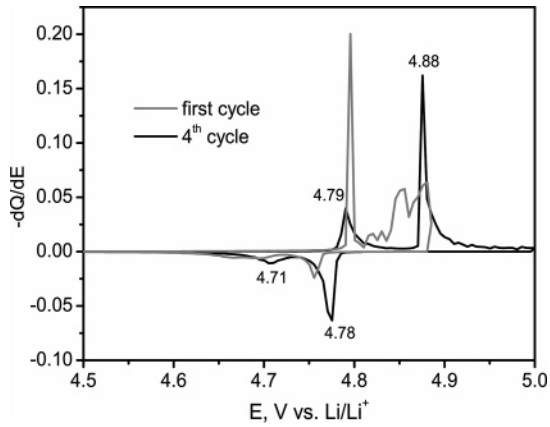

Figure 3. Potentiodynamic cycling with I_{lim} close to *C*/30 ($\Delta E = 5$ mV).

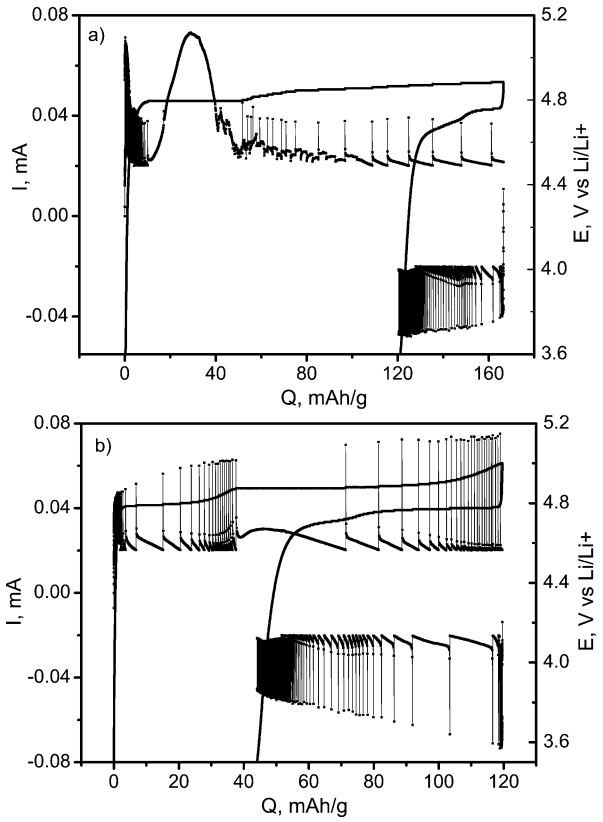

Figure 4. Current evolution in PITT experiment with I_{lim} close to *C*/30 during the (a) first cycle and (b) fourth cycle.

The current evolution during voltage steps in the PITT experiment with I_{lim} close to *C*/30 is shown in panels a and b of Figure 4 for the initial and the fourth cycles, respectively. In the first cycle, the parasitic reaction appears more pronounced than in the following cycles. The large peak of current, corresponding to the first plateau in the voltage−composition curve, is present in the first cycle only. Levi et al. proposed that this peculiar shape of current transient is characteristic for a slow nucleation step in a solid-state first-order phase transition.[24] A similar form of current response was reported for initial stages of lithium extraction from $LiCoO_2$[25] and for magnesium intercalation into Mo_6S_8.[24] Nevertheless, we cannot exclude that this form of current transient is due to the contribution from a parasitic reaction.

(24) Levi, M.; Lancry, E.; Gizbar, H.; Gofer, Y.; Levi, E.; Aurbach, D. *Electrochim. Acta* **2004**, *49*, 3201.

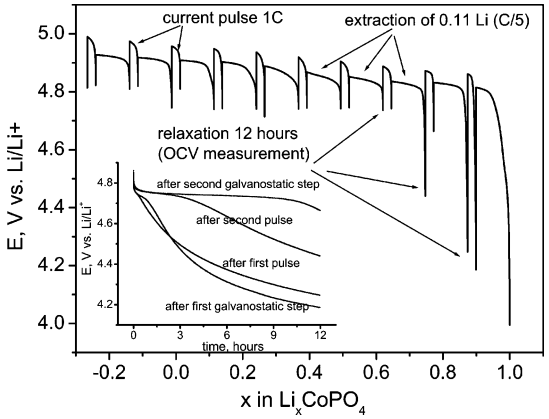

Figure 5. Voltage−composition curves taken in GITT charge (the protocol: charge 30 min *C*/5 corresponding to the extraction of 0.11 Li, relaxation for 12 h, current pulse 1*C* corresponding to the extraction of 0.02 Li, relaxation for 12 h).

Additionally, in the middle of charging, the current decays not monotonously and side reactions might occur. The current transients in the first and second voltage plateaus in the fourth cycle are characteristic for a two-phase transition. On the basis of a current transient analysis, we can propose a narrow solid solution domain for the initial stage of charge, corresponding to the extraction of ∼0.07 Li per mol $LiCoPO_4$, and at the end of discharge. Nevertheless, because of possible electrolyte decomposition, the interpretation of current decays is quite dubious as well as the detailed determination of domain extensions in terms of the lithium content. It should be noted that in the second and following cycles the difference between charge and discharge capacities results in a negative value for the calculated lithium content in the cathode, which has no physical meaning.

To reveal the equilibrium voltages at different stages of deintercalation, we performed a GITT experiment. Figure 5 illustrates the dependence of voltage versus composition obtained in a galvanostatic step experiment. After the galvanostatic step corresponding to the extraction of 0.11 Li, the open-circuit voltage of the cell was recorded for 12 h. A short current pulse (0.02 Li) was then applied and the open circuit voltage was recorded again for 12 h. At the initial stages of deintercalation, the drop of voltage during relaxation periods is very pronounced. It is quite unlikely that this drastic decrease in the voltage can be attributed to a high polarization at the beginning of charge, because the voltage transients (see inset in Figure 5) show the voltage plateaus before the voltage drops. These plateaus are very short after the first galvanostatic step and the first galvanostatic pulse, becoming more pronounced after the second galvanostatic step. In our opinion, this behavior indicates self-discharge of the cell due to the reaction of highly oxidative surface of the cathode with the electrolyte. In the early stages of charge, the amount of lithium deintercalated is low and the relaxation periods for 12 h are sufficient to reveal self-discharge of the cell. After two galvanostatic steps, we observed no voltage drops anymore at the end of the relaxation periods.

(25) Morcrette, M.; Vaughan, G.; Chabre, Y.; Tarascon, J.-M. www.biologic.info/Electrochemistry/Application note.

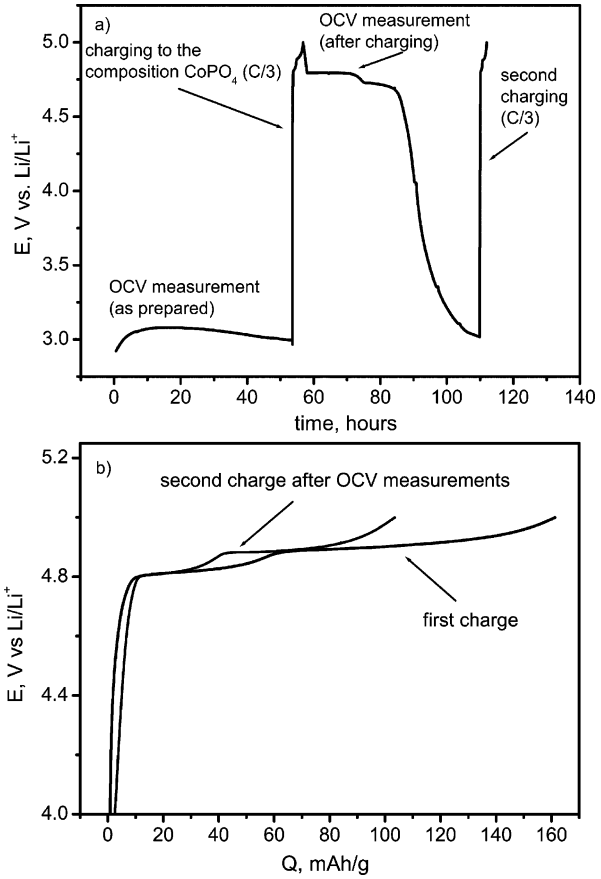

Figure 6. (a) OCV measurements for the cell before and after charging and (b) voltage−capacity curves for the first and second charging.

To provide more insight in this process, we charged the cell galvanostatically to the composition "$CoPO_4$", as calculated from the electrochemical data and recorded the open-circuit voltage for a few days (Figure 6a). Additionally the impedance spectra were recorded during the relaxation periods before and after charging (Figure 7a, b). The pristine cell exhibits one semicircle in the high-frequency region followed by a Warburg contribution at low frequencies (Figure 7a). After a relaxation period of 6 h, the impedance of the freshly prepared cell increases slightly and does not show any significant changes after that. The relaxation of the charged cathode is accompanied by a stepwise change of the open-circuit voltage (Figure 6a) and an increase in the cell impedance (Figure 7b). The existence of two plateaus during relaxation, very similar to the galvanostatic discharge curve, is an indication of self-discharge proceeding as

$$\text{“CoPO}_4\text{”} + \text{Li}^+ + \text{electrolyte (reduced form)} \rightarrow \text{LiCoPO}_4 + \text{electrolyte (oxidized form)}$$

In this case, the prolonged relaxation should lead to the formation of the pristine compound, from which lithium can be extracted again. In fact, charging the cell again after the relaxation period reveals the two plateaus in the charge curve that are characteristic for this compound (Figure 6b).

If the insertion of lithium proceeds via decomposition of the electrolyte, the products of the electrolyte decomposition can contribute to the surface film formation on the cathode side. The medium-frequency semicircle is usually attributed

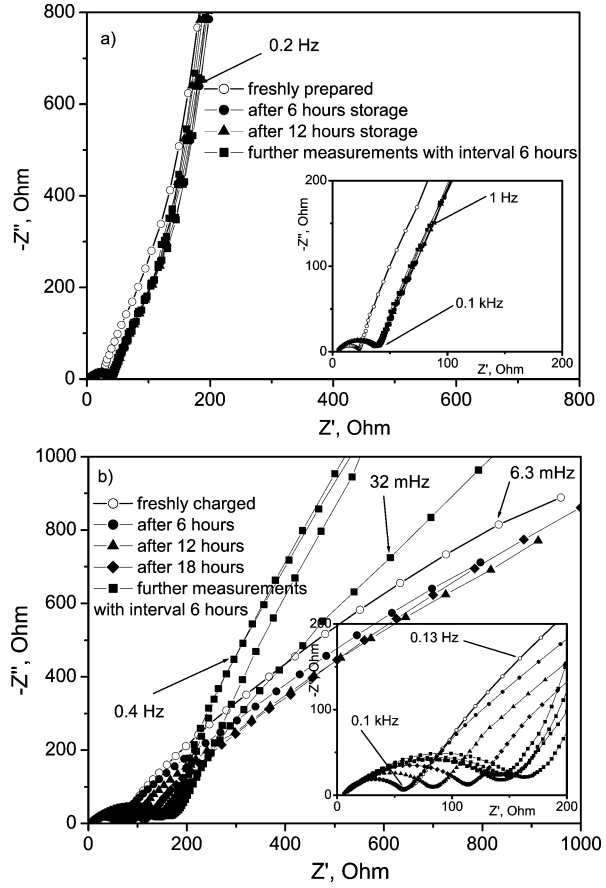

Figure 7. Nyquist plot for the $LiCoPO_4$ cell (a) before and (b) after charging.

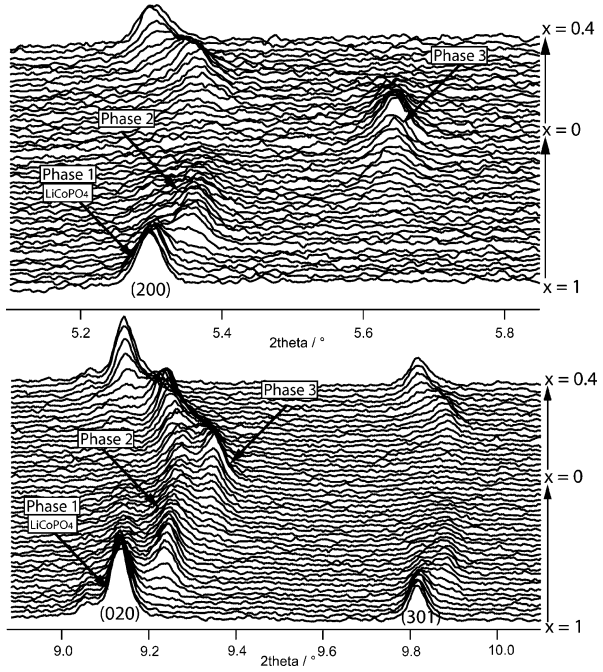

Figure 8. Selected regions in the diffraction patterns taken in situ during the first charge−discharge cycle. 200, 020, and 301 reflections are shown ($\lambda = 0.47189$ Å).

to Li-ion migration through the surface film and the charge transfer at the interface coupled with the double layer capacitance. It is reasonable to assume that the increase in the medium-frequency semicircle is due to the surface film growth (see Figure 7b).

To elucidate the structural transformations occurring at different stages of extraction−insertion, we performed in-situ synchrotron diffraction. As previously reported,[11] an ex situ recorded diffraction pattern of this sample, charged to the composition "$CoPO_4$", revealed reflections from two olivine-like phases with different cell volumes and a strong contribution from an amorphous fraction of the sample. We supposed that the cathode undergoes amorphization upon lithium extraction.

Figure 8 shows the evolution of selected reflections in the synchrotron diffraction patterns during charge−discharge of the cell at a *C*/12 rate. No amorphization of the active compound was observed in the in situ measurements. In the initial stage of charge, the formation of a second olivine-like phase is indicated by the appearance of a second set of reflections, e.g., 200, 020, and 301 in Figure 8, slightly shifted with respect to those from pristine $LiCoPO_4$. This is consistent with previous reports on $LiCoPO_4$ delithiation.[1,11] The lattice parameters of this new phase 2 ($a = 10.070(3)$ Å, $b = 5.851(2)$ Å, $c = 4.717(2)$ Å) determined for the diffraction pattern corresponding to the extraction of 0.3 Li per formula unit of $LiCoPO_4$ are very close to those of pristine $LiCoPO_4$ ($a = 10.1955(8)$, $b = 5.9198(5)$, $c = 4.6971(4)$ Å) obtained from Rietveld refinement. After approximately 0.3 Li per formula unit of $LiCoPO_4$ is extracted (corresponding to the end of the first plateau in Figure 1), the reflections of a phase 3 appear. The increasing intensity of these reflections (phase 3) is accompanied by the decreasing intensity of the reflections from phase 2. This transformation is not complete at the end of charge, and the reflections from phase 2 are still present after the extraction of one lithium from $LiCoPO_4$ (as calculated from the electrochemical data). This is proof that some parasitic reactions contribute slightly to the charge passed through the cell and result in the discrepancy between calculated and "real" lithium content in the cathode. During discharge, the transformation of the reflections proceeds in opposite directions in a reversible manner. The reflections of phase 3 disappear completely at the end of discharge, and the diffraction pattern at this stage is quite similar to the one of the pristine compound. Nevertheless, at the end of discharge, the reflections are slightly broader in comparison to the pristine compound.

To reveal the structure of phase 3, appearing upon charging the cell, we overcharged the in situ cell in a separate test. In this case, the in situ charging was performed without voltage limitation until no further changes in the diffraction pattern could be detected. Under these conditions, we obtained phase 3 almost as the only crystalline product of deintercalation, with only weak additional reflections from phase 2. The reflections of phase 3 could be indexed on the basis of an orthorhombic unit cell ($a = 9.567(2)$ Å, $b = 5.7806(9)$ Å, $c = 4.7636(9)$ Å). Rietveld refinement confirmed that phase 3 has the same olivine-like structure as the pristine compound (see Figure 9).

The formation of phase 3 upon lithium extraction from $LiCoPO_4$ has not been reported before. The only product of deintercalation was pointed out to be phase 2 with an ill-defined lithium content. We believe that phase 3 is $CoPO_4$

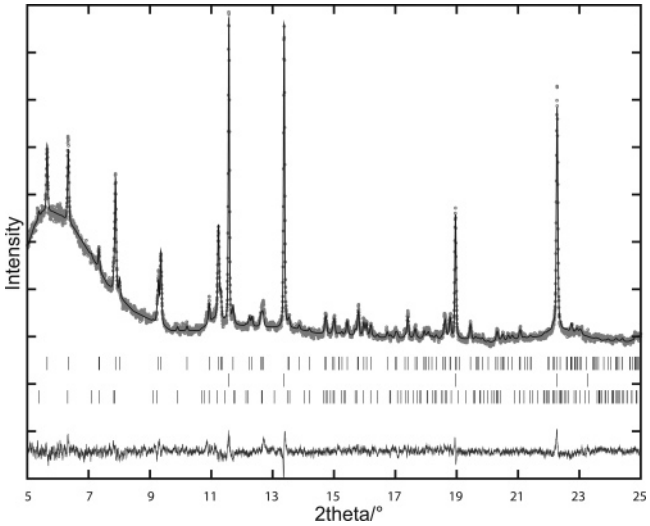

Figure 9. Experimental and calculated patterns and their difference for $LiCoPO_4$ charged to the composition "$CoPO_4$" ($\lambda = 0.47189$ Å). The positions of the reflections are shown from top to bottom: phase 3, Al from the setup (current collector on the cathode side), phase 2. The initial atomic coordinates for phase 2 and phase 3 were taken from the $LiCoPO_4$ structure; atomic coordinates for phase 3 were refined. A profile matching was applied for the Al contributions. The phase ratio was found to be 90-(3)% of phase 3 and 10(1)% of phase 2.

with an olivine-like structure, which is unstable in air but can be recovered under in situ conditions. In fact, the diffraction pattern of the charged cathode measured after dissembling the cell is characteristic for an amorphous sample with weak reflections from phase 2.

Until now, there have been no references concerning experimentally prepared $CoPO_4$. In the theoretical work of Osorio-Guillen et al., the unit-cell volume for $CoPO_4$ with olivine structure was predicted to be 275.83 Å^3 (ICSD ref 99863) on the basis of DFT calculations.[26] On the other hand, another DFT analysis with local density approximation resulted in a cell volume for orthorhombic $CoPO_4$ of 260 Å^3.[27] This value is quite close to the observed unit-cell volume of phase 3 (263.43(8) Å^3).

The phase appearing at the early stage of charge (phase 2) is an olivine-like phase with $0 \leq x \leq 1$ in Li_xCoPO_4. Because of the low scattering factor of lithium for X-rays, the amount of lithium could not be deduced from a refinement of the occupation factor on the Li site. On the basis of the extension of the first plateau in the voltage−composition curves, we believe that the lithium content in phase 2 should be close to $x = 0.7$. Additionally, we compared the experimental unit-cell volumes reported for the pristine $LiMPO_4$ (M = Co, Fe, Mn) and their delithiated forms MPO_4 (see Figure 10). Assuming that phase 3 is the olivine-like $CoPO_4$, we obtain a difference in the cell volumes of about 7%, which is practically the same as for $LiFePO_4$/$FePO_4$. The cell volume of phase 2 (277.94(14) Å^3) in this plot corresponds to a composition $Li_{0.7}CoPO_4$, if a linear correlation between lithum content and the unit-cell volume is applied.

The cell parameters for all olivine-like phases observed during in situ measurements are summarized in Table 1. The

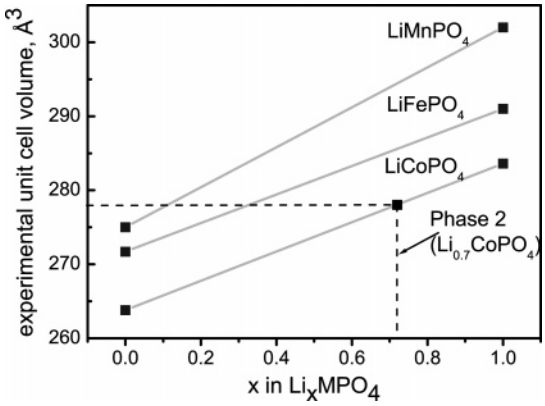

Figure 10. Comparison of the observed unit cell volumes for orthorhombic $LiMPO_4$ and their delithiated forms MPO_4. The experimental data for $LiMnPO_4$/$MnPO_4$ were taken from ref 7; for $LiFePO_4$/$FePO_4$, from ref 6.

Table 1. Unit-Cell Parameters for Three Olivine-Like Phases $LiCoPO_4$ (phase 1), $Li_{0.7}CoPO_4$ (phase 2), and $CoPO_4$ (phase 3) (space group *Pnma*)

	a (Å)	*b* (Å)	*c* (Å)	*V* (Å^3)
$LiCoPO_4$	10.1955(8)	5.9198(5)	4.6971(4)	283.49(4)
$Li_{0.7}CoPO_4$	10.070(3)	5.851(2)	4.717(2)	277.94(14)
$CoPO_4$	9.567(2)	5.7806(9)	4.7636(9)	263.43(8)

atomic coordinates for $Li_{0.7}CoPO_4$ were taken from pristine $LiCoPO_4$ and not refined. The atomic coordinates for $CoPO_4$ were refined with the diffraction pattern collected from the overcharged in situ cell. The atomic coordinates and characteristic interatomic distances are summarized in table 2 and 3, respectively.. For the complete set of in situ diffraction data scale factors, *U* and *W* parameters, cell constants, and background points were refined.

The unit-cell volumes (Figure 11) demonstrate no significant changes upon cycling that support the idea that the extraction−insertion of lithium proceeds via the coexistence of different olivine-like phases, each with a constant lithium content. Nevertheless, in the beginning of deintercalation, the two initial diffraction patterns were fitted with the structure model of phase 1, because the reflections from phase 2 are not yet visible. Therefore, a narrow solid−solution region cannot be excluded for the initial extraction of ~0.05 Li per mol of $LiCoPO_4$. The current transients in a PITT experiment also indicated the existence of a solid−solution domain at the beginning of the extraction. Additionally, at the end of discharge, the cell volume of phase 2 increases, approaching the cell volume of phase 1. This change in cell volume may indicate that at the end of discharge, the two-phase mechanism changes into a single-phase reaction. On the basis of this data, we can speculate that extraction−insertion of lithium from $LiCoPO_4$ includes a narrow solid−solution domain close to the end members, similar to the mechanism proposed for $LiFePO_4$ by Yamada et al.[8,9]

The evolution of the phase ratios obtained from the Rietveld refinement (Figure 12a) is compared with the "theoretical" phase ratio, calculated for a stepwise transformation of $LiCoPO_4$ to $Li_{0.7}CoPO_4$ and $Li_{0.7}CoPO_4$ to $CoPO_4$ (Figure 12b). First, one can see the significant discrepancy between lithium content calculated from electrochemical data and lithium content deduced from the refinement at the end of charge. Reflections from pristine $LiCoPO_4$ and phase 2

(26) Osorio-Guillen, J. M.; Holm, B.; Ahuja, R.; Johansson, B. *Solid State Ionics* **2004**, *167*, 221.
(27) Le Bacq, O.; Pasturel, A.; Bengone, O. *Phys. Rev. B* **2004**, *69*, 245107.

Table 2. Positional Parameters for the Three Olivine-Like Phases Observed during Lithium Extraction−Insertion. Refined Parameters Are Given with Estimated Standard Deviations in Brackets

	$LiCoPO_4$			$Li_{0.7}CoPO_4$			$CoPO_4$		
	x/*a*	*y*/*b*	*z*/*c*	*x*/*a*	*y*/*b*	*z*/*c*	*x*/*a*	*y*/*b*	*z*/*c*
Li	0.5	0.5	0.5	0.5	0.5	0.5			
Co	0.2792(5)	0.25	0.9796(15)	0.2792	0.25	0.980	0.2707(9)	0.25	0.9457(18)
P	0.0950(5)	0.25	0.418(2)	0.0950	0.25	0.418	0.0869(18)	0.25	0.3871(39)
O(1)	0.093(3)	0.25	0.740(5)	0.093	0.25	0.740	0.122(4)	0.25	0.716(7)
O(2)	0.452(3)	0.25	0.204(5)	0.452	0.25	0.204	0.444(4)	0.25	0.151(7)
O(3)	0.167(2)	0.043(3)	0.284(3)	0.167	0.043	0.284	0.166(3)	0.029(5)	0.244(5)

Table 3. Bond Distances for Pristine $LiCoPO_4$ and Delithiated Phase $CoPO_4$

$LiCoPO_4$		$CoPO_4$	
Co(1)−O(1)	2.207(29)	Co(1)−O(1)	1.795(38)
Co(1)−O(2)	2.053(29)	Co(1)−O(2)	1.925(38)
Co(1)−O(3)	2.038(18)×2	Co(1)−O(3)	1.973(28)×2
Co(1)−O(3)	2.203(18)×2	Co(1)−O(3)	2.157(28)×2
P(1) -- O(1)	1.513(25)	P(1) -- O(1)	1.602(38)
P(1) -- O(2)	1.567(30)	P(1) -- O(2)	1.379(42)
P(1) -- O(3)	1.561(18)×2	P(1) -- O(3)	1.634(30)×2
Li(1)−O(1)	2.140(19)×2		
Li(1)-O(2	2.089(17)×2		
Li(1)−O(3)	2.178(18)×2		

are still present at this stage, although all lithium should be extracted from the cathode on the basis of the electrochemical charge flown. The observed phase ratio of 73(1)% $CoPO_4$, 18(1)% $Li_{0.7}CoPO_4$, and 8.0(4)% $LiCoPO_4$ corresponds to 20% residual lithium remaining in the cathode. Thus, the combination of in situ diffraction and electrochemical data reveals unambiguously the parasitic reaction of the electrolyte decomposition. Second, at the beginning of charge, a two-phase coexistence is clearly identified. Before this transformation is completed, reflections from the phase 3 ($CoPO_4$) appear; all three phases then coexist up to the end of charge. The growth of the phase 3 is accompanied by the simultaneous decrease in the contents of both phases $LiCoPO_4$ and $Li_{0.7}CoPO_4$. It points out the kinetic limitations upon initial phase transformation and therefore supports the assumption that the initial delithiation of $LiCoPO_4$ proceeds with lower kinetics in comparison to the following cycles. The phase ratio upon discharge is characteristic for stepwise phase transitions: $CoPO_4$ to $Li_{0.7}CoPO_4$ and $Li_{0.7}CoPO_4$ to $LiCoPO_4$.

Conclusion

We have shown that the two plateaus in the charge−discharge curves, characteristic for $LiCoPO_4$, are related to two two-phase regions. The two olivine-like phases appearing at different stages of extraction−insertion were identified with in situ synchrotron diffraction. The existence of an intermediate state contradicts with the mechanism previously reported for this compound and differs from the mechanism known for $LiFePO_4$ and $LiMnPO_4$. We propose that lithium extraction from $LiCoPO_4$ leads to the formation of $Li_{0.7}CoPO_4$ and then to the formation of $CoPO_4$. Upon lithium insertion, the phase transitions proceed in the opposite direction. Because of the amorphization of the completely delithiated compound in air, this phase can only be detected under in situ conditions. This phase was not observed in our previous in situ measurements,[11] probably because of incomplete charging of the cell and parasitic reactions, resulting in a too low degree of charge.

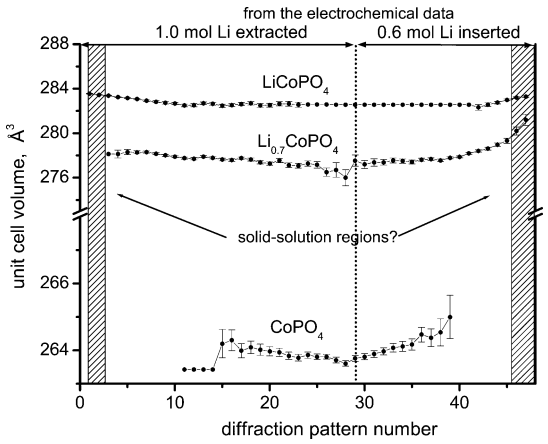

Figure 11. Experimental unit-cell volumes for the olivine-like phases observed during in situ cycling.

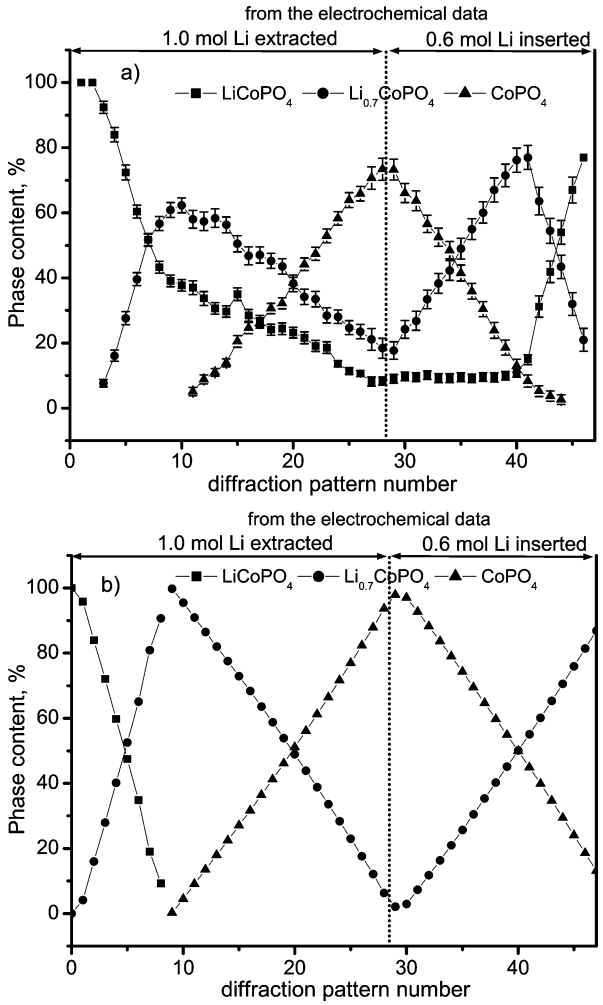

Figure 12. Phase ratio (a) obtained from Rietveld refinement and (b) calculated from electrochemical data, under the assumption that lithium extraction proceeds as two two-phase transitions $LiCoPO_4$−$Li_{0.7}CoPO_4$ and $Li_{0.7}CoPO_4$−$CoPO_4$.

The lithium stoichiometry in lithium-deficient olivine-like phases appearing upon lithium extraction from $LiCoPO_4$ cannot be confirmed by Rietveld analysis because of the low photon scattering cross-section of lithium. Unfortunately, because of parasitic reactions, the determination of the stoichiometry from the plateaus in the voltage−composition curves is also not very reliable. Nevertheless, the comparison of the cell volumes for the lithiated and delithiated forms of cobalt and iron olivine-like phosphates confirms these stoichiometries for the lithium-poor phases. However, the stoichiometries of the delithiated phases have to be proven by additional techniques, especially by neutron diffraction.

We believe that the two-step mechanism of lithium extraction is characteristic for $LiCoPO_4$ and independent from the preparation method. Nevertheless, the voltages corresponding to the first and second step are very close to each other, and voltage separation can be masked by polarization effect and/or by parasitic reactions, e.g., we have already shown that the two steps in the voltage−composition curve are not pronounced for the sample prepared at high temperature, consisting of 5−10 μm big crystallites.[11] The ball-milling of this sample was shown to enhance the electrochemical performance and result in the better resolution of two steps upon galvanostatic cycling. Additionally, lowering of the annealing temperature and, hereby, particle size was found to improve the separation of the two steps in the charge−discharge curves for this compound. The different reports in literature about the character of the voltage−composition curves (one-step versus two-step behavior) is probably due to different particle sizes and/or morphologies of the samples.

The initial delithiation seems to be kinetically hindered, so that a region with coexistence of three olivine-like phases is observed upon the first charge. The evolution of the diffraction patterns during discharge is characteristic for two stepwise phase transitions. The question remains whether solid−solution domains upon delithiation−lithiation of $LiCoPO_4$ really exist. The electrochemical examination with conventional battery electrolytes is jeopardized by parasitic reactions and/or by self-discharge of the cell. In our opinion, a more reliable conclusion can be drawn from structural study of chemically delithiated samples.

In situ diffraction, in combination with electrochemical techniques, revealed a significant contribution of the parasitic reaction to the electrochemical charge. This reaction can be attributed to the oxidative decomposition of the electrolyte. The improvement of oxidative stability of the electrolyte is a crucial point for achieving a high cycling stability for this cathode material.

Acknowledgment. This work was financially supported by the Deutsche Forschungsgemeinschaft in the frames of priority program SPP 1181, Grant DFG EH 183/3. Dedicated setups for the in situ characterisation of polycrystalline materials were developed by the Virtual Helmholtz Institute VH-VI-102.

CM062246U